Optics Communications 282 (2009) 1969–1972

Contents lists available at ScienceDirect

Optics Communications

journal homepage: www.elsevier.com/locate/optcom

2.1 Tesla permanent-magnet Faraday isolator for subkilowatt average power lasers

Ivan Mukhin *, Alexandr Voitovich, Oleg Palashov, Efim Khazanov

Institute of Applied Physics, Russian Academy of Sciences, 46 Ulyanov Str., 603950 Nizhny Novgorod, Russia

ARTICLE INFO

Article history:
Received 1 September 2008
Received in revised form 3 February 2009
Accepted 5 February 2009

Keywords:
Faraday isolator
Isolation degree
Thermally induced birefringence
Thermal lens

ABSTRACT

A Faraday isolator with one magneto-optical element providing 31 dB isolation ratio for 330 W average power lasers was produced and investigated in an experiment. These remarkable parameters were achieved by increasing the magnetic field and using a [001] oriented TGG crystal.

1. Introduction

A constantly growing average power of pulsed-periodic and CW lasers makes the problem of improving optical devices increasingly more topical, the key demand being suppression of thermally induced effects due to radiation absorption. Among the devices subject to thermal self-action are Faraday isolators (FI) by virtue of the relatively high ($\sim 10^{-3}$ cm^{-1}) absorption in magneto-optical elements (MOE) [1–3]. Temperature distribution that is nonuniform over the MOE cross-section gives rise to temperature distortions (thermal lens), nonuniform distribution of the angle of rotation of polarization plane caused by temperature dependence of Verdet constant, mechanical stress and, as a consequence, to linear birefringence (photoelastic effect) [4]. The degree of FI isolation is determined by depolarization caused by the photoelastic effect, and the contribution of the temperature dependence of Verdet constant is negligibly small [4,5]. Thus, as the radiation power is increased, the isolation ratio reduces. Consequently, for a given isolation ratio, average power of radiation passing through the FI cannot exceed the maximal value P_{max}. For commercial FIs, the characteristic magnitude is $P_{max} \cong 100$ W for the isolation ratio of 30 dB.

There are different ways of increasing P_{max}. For example, partitioning of a magneto-active element into thin disks cooled through an optical surfaces [6]. Such geometry leads to substantial reduction of the transverse temperature gradient, hence, to a decrease of thermal distortions in the disks. Another popular method [4,7–9] is based on the compensation of thermal depolarization. For this, one magneto-optical element rotating the polarization plane by 45° is replaced by two elements, with a reciprocal optical element placed between them. The distortions arising during passage through the first element are partially compensated in the transmission through the second element. The FIs based on this idea ensure reliable isolation for kilowatt transmitted radiation power [10,11]. It is reasonable to use for kilowatt (and higher) power a cryogen FI [12–14] and a FI with a superconducting solenoid as a magnetic system [13]. The methods of increasing P_{max} described above have drawbacks associated with bulky design and costly FI. At the same time, we believe that the potential of a traditional scheme with one MOE has not been fully exhausted.

By depolarization γ we understand the relation

$$\gamma = \frac{P_1}{P_1 + P_2}, \tag{1}$$

where $P_{1,2}$ are the depolarized and principal polarized components of radiation, respectively, and isolation ratio (degree of isolation) I measured in decibel is defined by

$$I[\mathrm{dB}] = 10 \cdot \log \frac{1}{\gamma}. \tag{2}$$

The depolarization γ caused by radiation absorption in optical elements of the FI and referred to as "hot" or "thermally induced" depolarization depends on the optical radiation power, as well as on the length, geometry, and material constants of MOE. The depolarization depends on a crystal orientation because of anisotropy of photoelastic effect. It is shown in Ref. [8], that the best orientation from the point of view of the minimal depolarization in the FI is the [001] orientation. For a cubic crystal having orientation [001] we have [4]

* Corresponding author.
E-mail address: mib_1982@mail.ru (I. Mukhin).

0030-4018/$ - see front matter
doi:10.1016/j.optcom.2009.02.008

$$\gamma_{001} = A_0 p^2, \tag{3}$$

where

$$p = \frac{Q\alpha L P_L}{\lambda\kappa}, \quad Q = \alpha_T \frac{n_0^3}{4} \cdot \frac{1+\nu}{1+\nu}(p_{11} - p_{12}), \tag{4}$$

λ and P_L are the wavelength and the radiation power; L, α, κ, p_{ij}, α_T, n_0 and ν are, respectively, the length, absorption coefficient, thermal conductivity, photoelastic coefficients, linear expansion coefficient, index of refraction and Poisson coefficient for the MOE material. For the Gaussian beam distribution, $A_0 = 0.014$. For a [1 1 1] cubic crystal [4],

$$\gamma_{111} = A_0 \left(\frac{1+2\xi}{3}\right)^2 p^2, \tag{5}$$

where $\xi = 2p_{44}/(p_{11} - p_{12})$ is the parameter of optical anisotropy. The medium with the minimal value $\alpha Q/\kappa V$ (V is the Verdet constant) is the optimal for high-power FI [12,15]. Such medium for radiation with wavelength about 1 μm is the TGG crystal. For TGG, $\xi = 2.25$. Therefore, as follows from (3)–(5) the use of a [0 0 1] crystal gives a pronounced increase of P_{max} (about two-fold) as compared to a crystal having orientation [1 1 1] that is most popular. To the best of our knowledge, all parameters of TGG crystal (Verdet constant, thermal conductivity, expansion coefficient) do not depend on crystal orientation due to cubic symmetry of the TGG crystal.

In the current work, we describe the FI with a traditional scheme that ensure decoupling of about 30 dB at laser radiation power up to $P_{max} = 400$ W. This relatively high P_{max} is determined by two factors. The first one is magnetic field increase. In Ref. [16,17] the systems on constant magnets with a magnetic field up to 1 T are designed. In Section 2, we will describe a magnetic system with a basically new design that allows one to increase the magnetic field more than 2 T and, as a consequence, to shorten the MOE down to 10.3 mm. The second factor is the use as a MOE of a TGG crystal having orientation [0 0 1]. Results of experimental studies of the FI are presented in Section 3.

2. Features of magnetic system design

A Faraday isolator is a magnetic system (MS) on constant magnets, with a magneto-optical element placed inside.

An increase of the MS magnetic field H is a complex task. First, an increase of H implies shortening of the magneto-optical element, which imposes additional requirements to transverse homogeneity of the magnetic field. Second, an increase of H demands building-up a mass of magnets, M, and reinforces the mutual demagnetizing action of the neighboring magnets. Moreover, when the required (calculated) distribution of magnetization vector is achieved in the MS, one has to overcome technological difficulties at the stage of element production and at the subsequent stage of MS assembling. Therefore, we assemble magnetic schemes using diagrams that are a compromise between a desired magnetization field and a feasibility of practical implementation.

Our magnetic systems are sets of axially and radially magnetized rings. The software developed by our group enables us to design systems consisting of an arbitrary number of rings and predict the magnitude of the field to an accuracy not worse than 1%. Besides, the software allows optimization of different MS parameters (for instance, external dimensions of the MS, magneto-optical element length, and others). As a result, using the described method we can create magnetic systems with the isolation ratio higher than 40 dB. The calculations demonstrate that a set of axially and radially magnetized rings makes it possible to form needed magnetic field configuration in the 0–1.5 T range. However, for effective production of magnetic fields of ~2 T and higher directions of the ring magnetization must be much more complicated.

We propose to replace part of the magnets around TGG by a magnetic conductor retaining the total volume of the MS. The total energy of the field of magnets will decrease, but careful selection of the shape and position of the magnetic conductor will allow a local increase of field intensity in the region of MOE location. The diagram of the magnetic system design is depicted in Fig. 1. The magnetic conductor consists of two parts: the external part that is a screen (Fig. 1d) closing magnetic lines of force of the poles of radially magnetized rings (Fig. 1a and c), and the internal part – a pole terminal (Fig. 1e) concentrating magnetic field lines near the MOE. CT−10 steel was taken for a magnetic conductor. The magnets were made of the Nd–Fe–B alloy: radially magnetized rings with residual induction $B_{r1} \approx 12$–13 kG and coercitive magnetization force $H_{c1} \approx 13$ kOe and axially magnetized ring with induction $B_{r2} \approx 10$ kG and coercitive force $H_{c2} = 27$ kE. The MS had the following parameters: diameter 132 mm, length 140 mm, mass 12 kg, maximal magnitude of magnetic field 21 kOe. The mass (and size) of magnet system was chosen to minimize TGG length based on numerical results presented on Fig. 2. As can be seen from

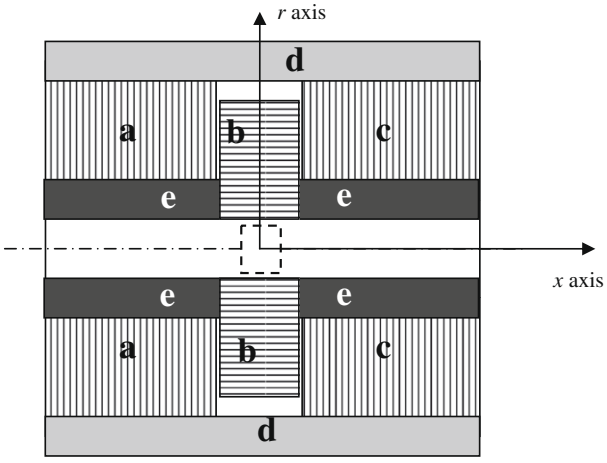

Fig. 1. Design of a magnetic system of FI. The horizontally hatched region b shows the axially magnetized ring (length is 24 mm, internal diameter is 15 mm, external diameter is 90 mm), the vertically hatched regions a and c show the radially magnetized rings (length is 58 mm, internal diameter is 27 mm, external diameter is 125 mm); the grey and black colors are for the magnetic conductor: regions d (length is 140 mm, internal diameter is 125 mm, external diameter is 132 mm) and e (length is 58 mm, internal diameter is 15 mm, external diameter is 27 mm). The broken lines show location of the TGG crystal.

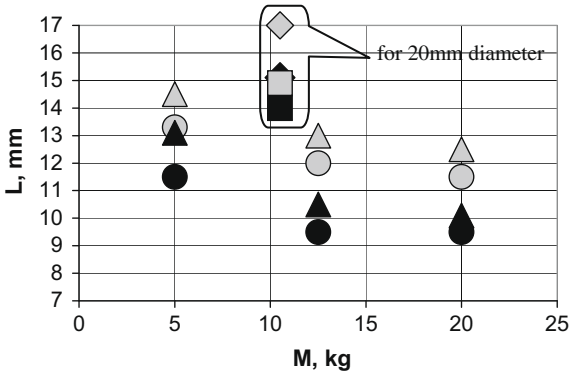

Fig. 2. Length L of a TGG crystal having diameter 13 mm (triangles and circles) and 20 mm (rhombs, squares) versus mass M of magnetic system with magnetic conductor (black symbols) and without it (grey symbols) for the isolation ratio of 30 dB (circles, rhombs) and 40 dB (triangles, squares).

Fig. 2 further increase of magnet mass and size gives almost nothing in terms of crystal length shortening.

Numerical calculations show that the central (axially magnetized) ring increases both the TGG length and isolation ratio induced by non-uniformity of magnet field, see Fig. 3. Hence, there is a tradeoff between these two major parameters of FI for high average power. Once the isolation ratio is defined, one can find the axially magnetized ring thickness for minimal crystal length, and hence minimal thermal effects. Typical isolation ratio induced by non-uniformity of magnet field is between 30 and 40 dB. For these two values we studied influence of magnet mass (and hence size) and magnet conductor on crystal length.

Results of measurements of magnetic field on the axis of the magnetic system of the studied FI are presented in Fig. 4. It is clear from this figure that on addition of the magnetic conductor the field in the center of the magnetic system grow from 1.7 to 2.1 T. Such a strong magnetic field enabled us to create a FI with the MOE length of 10.3 mm. The inhomogeneity H along r-axis was about 0.3%.

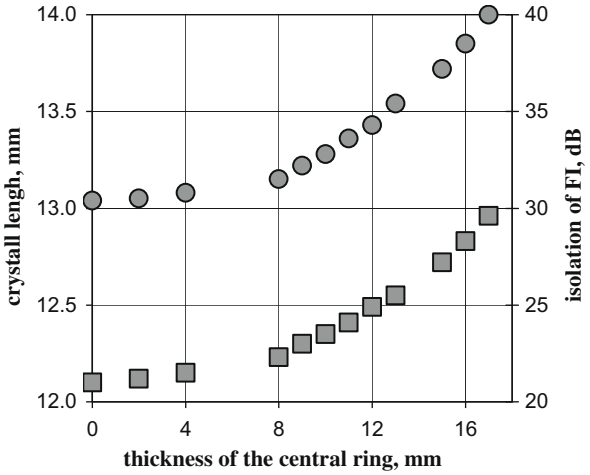

Fig. 3. The crystal length (circles) and isolation ratio of FI (squares) induced by non-uniformity of magnet field versus the thickness of the central ring in case of magnetic system without magnetic conductors.

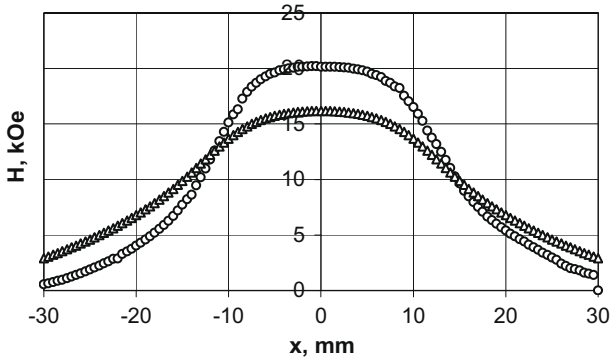

Fig. 4. Magnetic field magnitude in the studied FI with (circles) and without (triangles) magnetic conductor. The zero value along the x-axis corresponds to the center of magnetic system.

The length L of the TGG crystal 13 mm in diameter is shown in Fig. 2 as a function of mass M of the magnetic system with and without magnetic conductor. It is apparent from Fig. 2 that the magnetic conductor may have two functions. On the one hand, it ensures magnetic field enhancement in the region of a crystal conserving the degree of isolation, thanks to which the crystal may be shortened by ~20%. On the other hand, it provides additional increase of magnetic field homogeneity (for $M = 5$ kg a magnetic conductor increases the isolation ratio by 10 dB for almost unchanged L). To enhance isolation from 30 to 40 dB the crystal must be made a little longer, which corresponds to the transition from grey circles to grey triangles in the figure. At the same time, isolation by the same 10 dB may be achieved by means of a magnetic conductor, while the crystal length will decrease in this case. The values of the length L of a TGG crystal 20 mm in diameter for the magnetic system mass $M = 10.5$ kg are also shown in Fig. 3. In this case, the use of a magnetic conductor increases the isolation ratio from 30 to 40 dB at constant L, or it allows 7% (15%) shortening of the crystal length with retained isolation ratio of 30 dB (40 dB).

3. Optical characteristics of FI

The schematic of the experimental setup is shown in Fig. 5. CW linearly polarized radiation from a single-mode ytterbium fiber laser 1 at the wavelength of 1076 nm (produced by «IPG Photonics») was used as heating and probing radiation simultaneously. The maximum power of the beam 4.2 mm in diameter was 330 W. Radiation from laser 1 was coupled to the studied FI 2. Heating of MOE due to absorption resulted in depolarization of the radiation that was divided in the calcite wedge 3. The main portion of the radiation having power P_2 was coupled to the absorber 4, and the depolarized component having power P_1 was directed to the CCD camera 5. Rotation of the calcite wedge (Fig. 5) allowed us to control changes in the angle of rotation of the polarization plane with variation of the transmitted radiation power.

It is worthy of notice that γ may be fully determined by both, heat effects and "cold" depolarization that depends on the MOE quality and magnetic field inhomogeneity. In the MS of interest to us, the inhomogeneity H did not exceed <0.3%, which corresponds to cold depolarization $\gamma < 10^{-5}$. The depolarization as a function of the power of radiation transmitted through the FI is plotted in Fig. 6. In terms of maximal operating power P_{max}, the studied FI is 3–5 times better than the FI manufactured by leading companies. Besides, in the 100–500 W power range it may be regarded to be an alternative to the only available today operating FI scheme with depolarization compensation [4,10]. The broken line in Fig. 6 shows the theoretical dependence (3); the absorption was used as a fitting parameter ($\alpha = 2.5 \times 10^{-3}$ cm^{-1}). Here, we assumed $Q/\kappa = -3.5 \times 10^{-7}$ m/W [14] or $\kappa = 5$ W/km, $Q = 17 \times 10^{-7}$ K^{-1} [10]. If the absorption is reduced down to 10^{-3} cm^{-1}, then P_{max} will grow 2.5 times (see Fig. 6, the solid line).

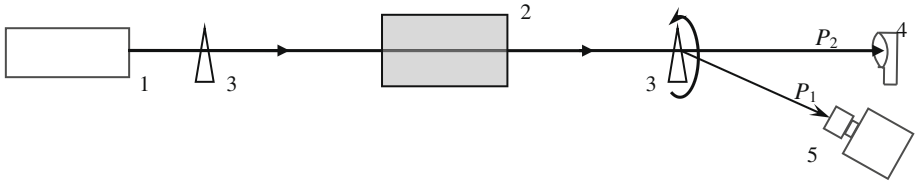

Fig. 5. Schematic of the experimental setup: 1 – ytterbium fiber laser, 2 – FI, 3 – calcite wedge, 4 – absorber, 5 – CCD camera.

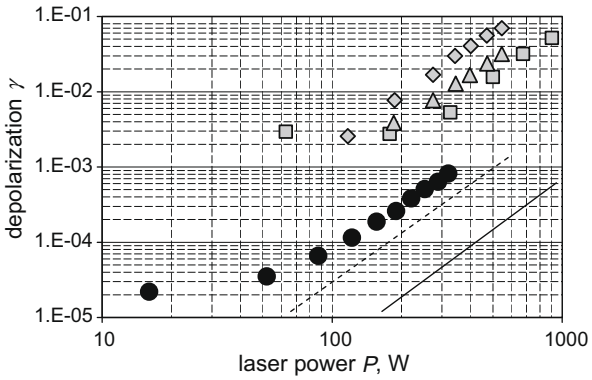

Fig. 6. Depolarization versus radiation power in the studied FI (black circles, broken line ($\alpha = 2.5 \times 10^{-3}\,cm^{-1}$), solid line is for ($\alpha = 10^{-3}\,cm^{-1}$) and in commercial FI produced by «Litton» (grey rhombs) [11], «Linos» (grey triangles) [11], and «EOT» (grey squares) [11].

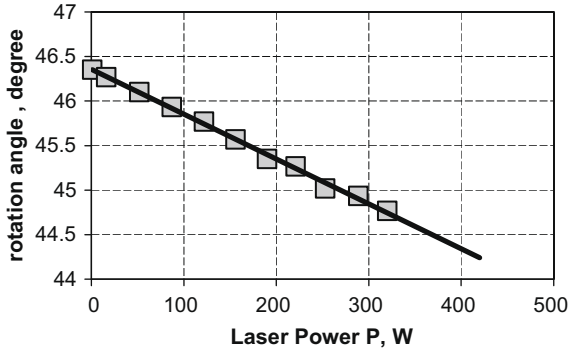

Fig. 7. FI angle of rotation versus laser power.

Another important characteristic of a FI is the angle of polarization rotation. During transmission of powerful radiation through the FI the MOE is heated, resulting in the decrease of the angle due to the temperature dependence of the Verdet constant. The influence of this effect on the isolation ratio may be eliminated by matching inclination of the polarizer axis [5]. At the same time, heating will inevitably result in increased losses at the first pass through the FI. It is seen in Fig. 7 that an increase in the radiation power from 0 to 400 W will lead to a decrease of the angle of rotation by 2°, which corresponds to losses in the FI at first pass of ~0.1% of radiation power. Note that this difficulty may be avoided by thermal stabilization of the MOE, for example, by means of the Peltier element.

The thermal lens focal length in the FI may be estimated by the formula from [19]:

$$F = \frac{4\pi\kappa a^2}{P_L L \alpha P}, \tag{6}$$

where P is thermo-optical constant [18] (for TGG $P/\kappa = -3.5 \times 10^{-6}$ m/W [18]) and a is the 1/e radius of a Gaussian beam. For the FI aperture of 13 mm, the Gaussian beam diameter must be ~5 mm. According to (6), for the radiation power of 400 W the focus of the parabolic component of the thermal lens will be ~23 m. Note that the thermal lens is stronger in the FI with compensated polarization distortions because the total length of the MOE is larger for the same magnetic field distribution inside the FI.

4. Conclusion

A Faraday isolator providing the isolation ratio of ~30 dB at average laser power of ~400 W was investigated in experiment. Such a high-power is ensured by two factors. First, the magnetic system has a basically new design that allows one to increase a homogeneous magnetic field up to 2.1 T and, hence, to shorten the MOE. Second, a [0 0 1] oriented TGG crystal is used as the MOE.

If still stronger magnets are used, it will be possible to make MOE still shorter and to additionally increase admissible optical power P_{max}. The estimates demonstrate a feasibility of producing FI on one disk MOE 13 mm in diameter and <7 mm long retaining the homogeneity of 30 dB. MOE shortening does not entail a significant increase of magnetic system dimensions for magnets having the following parameters: $B_{r1} \approx 14$ kG, $H_{c1} \approx 16$ kOe; $B_{r2} \approx 11.2$ kG, $H_{c2} = 35$ kOe [20]. Thus, the maximal field in the FI will equal 2.5 T. Besides there is an opportunity to use crystal TGG with the reduced absorption ($\alpha = 1.5 \times 10^{-3}\,cm^{-1}$ instead of $\alpha = 2.5 \times 10^{-3}\,cm^{-1}$). These two effects will allow increasing FI maximal power from 400 W up to 1 kW at 30 dB isolation ratio.

The work was done under support of The Foundation for Assistance to Small Innovative Enterprises (State Contract 4842p/7278).

References

[1] T.V. Zarubina, G.T. Petrovsky, Opticheskii zhurnal 59 (1992) 48.
[2] Research Institute of Materials Science and Technology, http://www.niimv.ru.
[3] Northrop Grumman, http://www.st.northropgrumman.com.
[4] E.A. Khazanov, Quantum Electronics 29 (1999) 59.
[5] E.A. Khazanov, O.V. Kulagin, S. Yoshida, D. Tanner, D. Reitze, IEEE Journal of Quantum Electronics 35 (1999) 1116.
[6] I.B. Mukhin, E.A. Khazanov, Quantum Electronics 34 (2004) 973.
[7] E.A. Khazanov, Quantum Electronics 31 (2001) 351.
[8] E. Khazanov, N. Andreev, O. Palashov, A. Poteomkin, A. Sergeev, O. Mehl, D. Reitze, Applied Optics 41 (2002) 483.
[9] N.F. Andreev, O.V. Palashov, A.K. Poteomkin, A.M. Sergeev, E.A. Khazanov, D.H. Reitze, Quantum Electronics 30 (2000) 1107.
[10] A.V. Voytovich, E.V. Katin, I.B. Mukhin, O.V. Palashov, E.A. Khazanov, Quantum Electronics 37 (2007) 471.
[11] K. Nicklaus, M. Daniels, R. Hohn, D. Hoffmann, in: Advanced Solid-State Photonics, Incline Village, Nevada, USA, 2006, p. MB7.
[12] D.S. Zheleznov, E.A. Khazanov, I.B. Mukhin, O.V. Palashov, in: Twelfth Conference on Laser Optics, St. Petersburg, 2006, p. TuR1.
[13] D.S. Zheleznov, E.A. Khazanov, I.B. Mukhin, O.V. Palashov, A.V. Voytovich, IEEE Journal of Quantum Electronics 43 (2007) 51.
[14] Ryo Yasuhara, Shigeki Tokita, Junji Kawanaka, Toshiyuki Kawashima, Hirofumi Kan, Hideki Yagi, Hoshiteru Nozawa, Takagimi Yanagitani, Yasushi Fujimoto, Hidetsugu Yoshida, Masahiro Nakatsuka, Optics Express 15 (18) (2007) 11255.
[15] M.J. Weber, in: L.G. DeShazer (Ed.), Laser and Nonlinear Optical Materials, Proc. SPIE, vol. 681, 1986, pp. 75–90.
[16] K. Shiraishi, F. Tajima, S. Kawakami, Optics Letters 11 (2) (1986) 82.
[17] Daniel J. Gauthier, Paul Narum, Robert W. Boyd, Optics Letters 11 (1986) 623.
[18] E.A. Khazanov, N.F. Andreev, A.N. Mal'shakov, O.V. Palashov, A.K. Poteomkin, A.M. Sergeev, A.A. Shaykin, V.V. Zelenogorsky, I. Ivanov, R.S. Amin, G. Mueller, D.B. Tanner, D.H. Reitze, IEEE Journal of Quantum Electronics 40 (2004) 1500.
[19] E. Perevezentsev, A. Poteomkin, E.A. Khazanov, Applied Optics 46 (2007) 774.
[20] Ningbo Permanent Magnetics Co., LTD., http://www.pm-magnets.com.